JOURNAL OF BACTERIOLOGY, July 1980, p. 89-99
0021-9193/80/07-0089/11$02.00/0

Vol. 143, No. 1

Positive Correlation Between Size at Initiation of Chromosome Replication in *Escherichia coli* and Size at Initiation of Cell Constriction

L. J. H. KOPPES AND N. NANNINGA*

Department of Electron Microscopy and Molecular Cytology, University of Amsterdam, Amsterdam, The Netherlands

The variability of (i) the length (size) at which cells initiate chromosome replication, (ii) the length at which they initiate cell constriction, and (iii) the time interval between these events has been estimated for *Escherichia coli* B/r K at two different slow growth rates. Steady-state cultures were pulse-labeled with [^{3}H]thymidine and, after fixation, analyzed by electron microscopic radioautography. The coefficient of variation of length at initiation of chromosome replication was found to be 15 to 22%, the coefficient of variation of length at initiation of cell constriction was 10%, and the coefficient of variation of the time interval between both events was 25%. With the help of these values we calculated a high positive coefficient of correlation (ρ) between the length at which a round of chromosome replication is initiated and that at which the onset of cell constriction occurs. At both growth rates ρ has a value of 0.6 to 1.0. This correlation excludes a model in which chromosome initiation and cell constriction are independently triggered by some aspects of cell growth. It favors a model in which an event before or at chromosome initiation triggers both.

During the bacterial cell cycle, chromosome replication and cell division are coordinated so that each daughter cell receives one complete genome at division (2, 4, 6, 15). For *Escherichia coli* B/r the interplay of chromosome replication and cell division is described in the Helmstetter-Cooper model (13). How coordination is achieved remains obscure, however.

The most direct way to study the cell cycle is to observe individual cells at successive times during growth by time-lapse photomicrography (7, 21, 29, 31, 33). However, the accuracy of this method is limited by the small size of bacteria, the small sample size, and the difficulty of maintaining steady-state growth conditions during the period of observation. An approach which avoids these problems is to infer the properties of individual cells from the distribution of sizes at which cell cycle events occur, or from the time variation of the periods between these events in a population which is in a steady state (3, 16–19, 26, 27). For instance, a small coefficient of variation (CV = 9.3%) has recently been reported for the period between successive rounds of DNA replication in rapidly growing *E. coli* B/r (26). This was compared with a CV of about 20% for the period between cell divisions (21, 29, 31, 33). On the other hand, the CV of size at initiation of DNA replication was found to be large (CV $\geq$ 15%) as compared to that (CV $\approx$ 10%) for size at cell division (16, 19).

In a previous paper dealing with size distributions at cell cycle events (see Fig. 6 in reference 19), we explained that the finding of a large CV for size at initiation of DNA replication and a small one for cell constriction (the standard deviations being similar) is compatible with two possibilities (Fig. 1). (i) The first possibility is that size at initiation of constriction is dependent on size at initiation of DNA replication (Fig. 1A). The size increment between these events (ΔL; hatched area) is about the same for both small (L_{i1}) and large cells (L_{i2}) at initiation of DNA replication. During exponential length growth (3, 7, 18, 19, 33; this paper), the smaller cells grow more slowly and need more time to increase with ΔL than the larger. This results in a distribution of the time interval between initiation of DNA replication and initiation of cell constriction (U period = C + D − T; see for symbols the lower part of Fig. 1), which is indicated by the dashed line in Fig. 1A.

(ii) The second possibility is that size at initiation of constriction is independent of size at initiation of DNA replication (Fig. 1B). Both small (L_{i1}) and large cells (L_{i2}) at initiation of DNA replication will initiate cell constriction at an average length L_c. As can be seen, individual cells that initiate chromosome replication at a small size (L_{i1}) have to accrue more (i.e., ΔL_1; hatched area) to reach L_c than cells (L_{i2}) that initiate at a large size (size increment: ΔL_2;

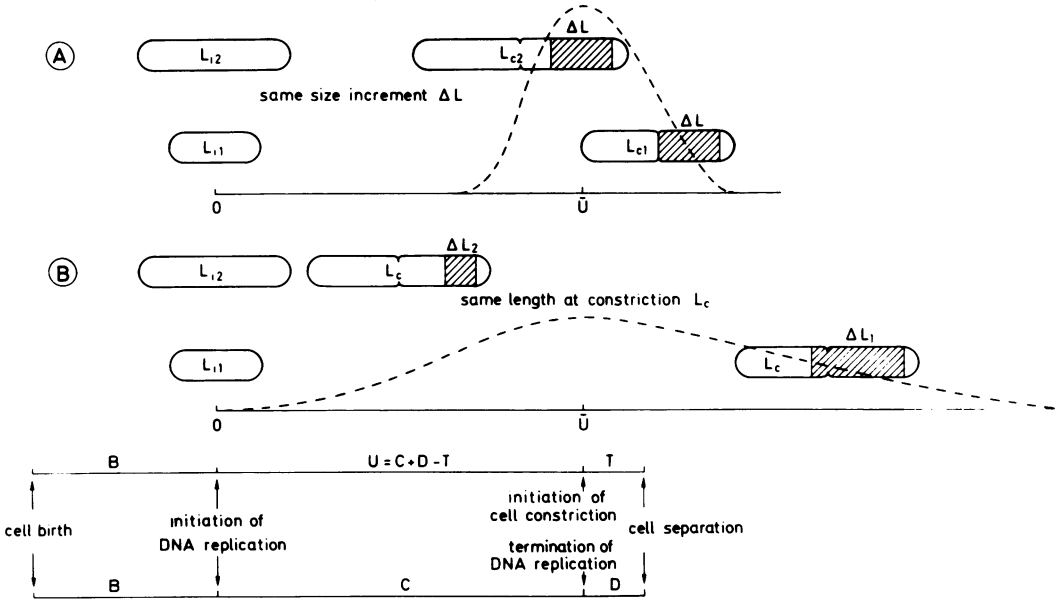

FIG. 1. *Two models for the coordination of DNA replication and cell division. The cells are assumed to elongate exponentially. (A) Length at initiation of constriction is dependent on length at initiation of DNA replication (positive correlation). Both small (L_{i1}) and large cells (L_{i2}) at initiation of DNA replication have increased with the length increment ΔL (hatched area) at initiation of constriction. (B) Length at initiation of constriction is independent of length at initiation of DNA replication (no correlation). Both small (L_{i1}) and large cells (L_{i2}) at initiation of DNA replication have on the average the same length at initiation of constriction (L_c). The expected distribution of the U period is indicated by the dashed lines. The symbols and the average duration of the periods of the cell division cycle are given in the lower part of the figure.*

hatched area). This leads to a more pronounced variation in the U period (dashed line) than for alternative (i).

Previously, we have chosen possibility (i) to explain our results with respect to the distribution of sizes at initiation of DNA replication and at initiation of constriction. To further distinguish between the two possibilities, we have made more detailed measurements, and we have in particular estimated the variation in the U period.

An exponentially growing culture of *E. coli* B/r K was pulse-labeled with [^{3}H]thymidine at two different growth rates. The CV of length at initiation of DNA replication was estimated by electron microscopic radioautography and found to exceed that at initiation of cell constriction (≥15% and 10%, respectively). The CV of the U period was determined from the fraction of constricted cells that were unlabeled at successive times after pulse-labeling during growth in nonradioactive medium, and was found to be about 25%. These results are compatible with size at initiation of constriction being dependent on size at initiation of DNA replication (Fig. 1A).

MATERIALS AND METHODS

Bacterial strain and growth conditions. The organism used was *E. coli* B/r K Thy$^-$, derived from the wild-type strain (obtained from H. Kubitschek) by trimethoprim mutagenesis. The strain was found to contain a small plasmid (M. Meyer, personal communication). The replication time of the plasmid is small compared to the duration of the pulse, so that, on the assumption of random replication of the plasmid during the cell division cycle, its contribution to the rate of DNA synthesis will be included in the correction made for aspecific background radioactivity. Because the results of the radioautographic analysis were not different from those of plasmid-free strains (see also reference 36), we believe that any effect of the plasmid on cell cycle parameters can be neglected. The strain was grown in a minimal medium (13) supplemented with 50 μg of thymine per ml and with, as carbon sources, either 0.2% L-alanine (doubling time, T_D = 180 min) or a mixture of 0.04% L-alanine and 0.04% L-proline (T_D = 90 min). For each experiment, 100 ml of minimal medium was inoculated with bacteria and incubated under aeration by shaking in a water bath at 37°C. Growth was monitored by measuring the absorbance at 450 nm with a Gilford spectrophotometer in samples fixed with 0.7% formaldehyde. This was done after 19 to 29 h of incubation, i.e., after about eight generations.

Pulse labeling with [^{3}H]thymidine. When the absorbance had reached a value of 0.5 (about 5×10^8 cells per ml), 1 ml of culture was fixed with 0.1% OsO_4 (unlabeled control), and 10 ml of culture was pulse-labeled with [^{3}H]thymidine (40 Ci/mmol; 50 μCi/ml; Radiochemical Centre, Amersham, England) during 5% of T_D.

The pulse was terminated by pouring the cells on a filter (pore size, 0.45 μm; filter diameter, 47 mm; Millipore Corp., Bedford, Mass.) and by washing with 100 ml of fresh, prewarmed medium with 0.5 mg of thymidine per ml. The duration of washing was 3% of T_D and has been included in the chase period. The labeled and washed cells were suspended in 50 ml of prewarmed growth medium and incubated with shaking in a water bath at 37°C. At successive times, 2-ml samples were fixed with 0.7% formaldehyde for the measurement of absorbance; 1-ml samples were fixed with 0.1% OsO_4, placed on ice, and then used for the determination of the fraction of unlabeled constricted cells (see below).

Agar filtration and radioautography. Agar filters were prepared as previously described (37). Both the unlabeled control cells and the pulse-labeled cells fixed at successive times during the chase were applied to the same filter (at different locations) in droplets of 10 μl. Bacitracin (1%) was added to promote spreading of the cells. The plastic film with adhering bacteria was floated off on distilled water and picked up from below with a glass slide previously covered with a collodion membrane. Contrast was enhanced by shadowing with platinum and carbon at an angle of about 60°. The slides were dipped in Ilford L4 emulsion diluted with 2 volumes of distilled water at 30°C with a semiautomatic apparatus. After an exposure of 16 days (T_D = 90 min) or 20 days (T_D = 180 min) at 4°C, the slides were developed for 15 min in Agfa-Gevaert developer (20): 0.75 g of Metol, 0.5 g of Na_2SO_3, and 0.2 g of KSCN in 100 ml of double-distilled water. The radioautograms were transferred to electron microscope grids and viewed in a Philips EM 300 electron microscope at a magnification of ×1,600.

Analysis of radioautograms. The average number of grains over radioactive cells was about five; the average number of background grains above non-radioactive cells in the control was less than 0.5. Therefore, cells were considered to be labeled when they were associated with at least two grains. For the construction of the "fraction of unlabeled constrictions" plot, at least 100 constricted cells from successive time samples were screened in the electron microscope. The constricted cells were scored as labeled or unlabeled.

The control sample and the samples that had been pulse-labeled and chased in non-radioactive medium for 0 and 40 min were also analyzed with respect to size. Areas were photographed at random, and the negatives were projected at a final magnification of 12,000 onto a transparent tablet digitizer (Summagraphics, Fairfield, Conn.), which was connected to a calculator (HP 9825A). The cell length, width, degree of constriction, and number of grains were determined with the digitizer, processed by the calculator, and stored on tape. Sample and theoretical length distributions were compared by means of the Kolmogorov-Smirnov test of goodness of fit (34) at a level of significance of 0.01 unless stated otherwise.

RESULTS

Comparison of control and treated cells. During the experiment we have checked whether changes occur in the mass doubling time (T_D) and in the length distributions of the various cell population samples. After pulse labeling with [^{3}H]thymidine, washing, and resuspension in a fresh non-radioactive growth medium, the absorbance increased without delay. The T_Ds during the chase (90 and 172 min) were well within experimental error from those of the parent culture before pulse labeling (93 and 180 min). The median generation times estimated from the fraction of unlabeled constrictions plot (i.e., the time after the pulse at which half of the constricted cells contained one labeled chromosome) were 92 min and 184 min, respectively.

Length distributions obtained from treated cells (0-min and 40-min chase) were found not to differ from untreated control cells (D_{max} = 7.2%; D_{krit} = 9.8%) in one case (T_D = 90 min) and only slightly (D_{max} = 7.8%; D_{krit} = 6.4%) in the other (T_D = 180 min). The difference between the average lengths of control and treated cells was less than 0.1 μm, which is within the reproducibility of measuring length distributions from the same sample. These data indicate a steady state of growth during the experiment.

Length distributions of newborn and separating cells. These distributions are required for the Collins and Richmond equation to calculate a relation between cell length and time. We distinguish separating cells from constricting cells because it takes some time before constriction is followed by separation. For the estimation of length at birth (L_0) and at cell separation (L_s), the constricted cells (hatched area in Fig. 2; parameters in Table 1) were classified by eye as slightly, medium, and very constricted. The average length was found to increase during constriction with a constant CV. Therefore, the lengths of the medium constricted cells, when multiplied with the factor $f = \bar{L}$ very constricted cells/$\bar{L}$ medium constricted cells ($1.04 < f < 1.09$), gave a distribution which did not differ significantly from that of the very constricted cells. The corrected distribution of the medium constricted cells and the distribution of the very constricted cells were pooled. The resulting distribution was used to estimate the distribution at cell separation [$\phi(x)$]; the distribution of the prospective daughters of the separating cells was used to estimate the distribution at birth [$\psi(x)$]. The parameters of the $\psi(x)$ and $\phi(x)$ distributions are shown in Fig. 2 (vertical lines) and in Table 2. Log normal fits to the estimated $\psi(x)$ and $\phi(x)$ distributions could not be rejected ($\alpha = 0.10$) and were routinely used in the further analysis for the sake of computational convenience.

From the $\psi(x)$ and $\phi(x)$ distributions we calculated theoretical length distributions $\lambda(x)$

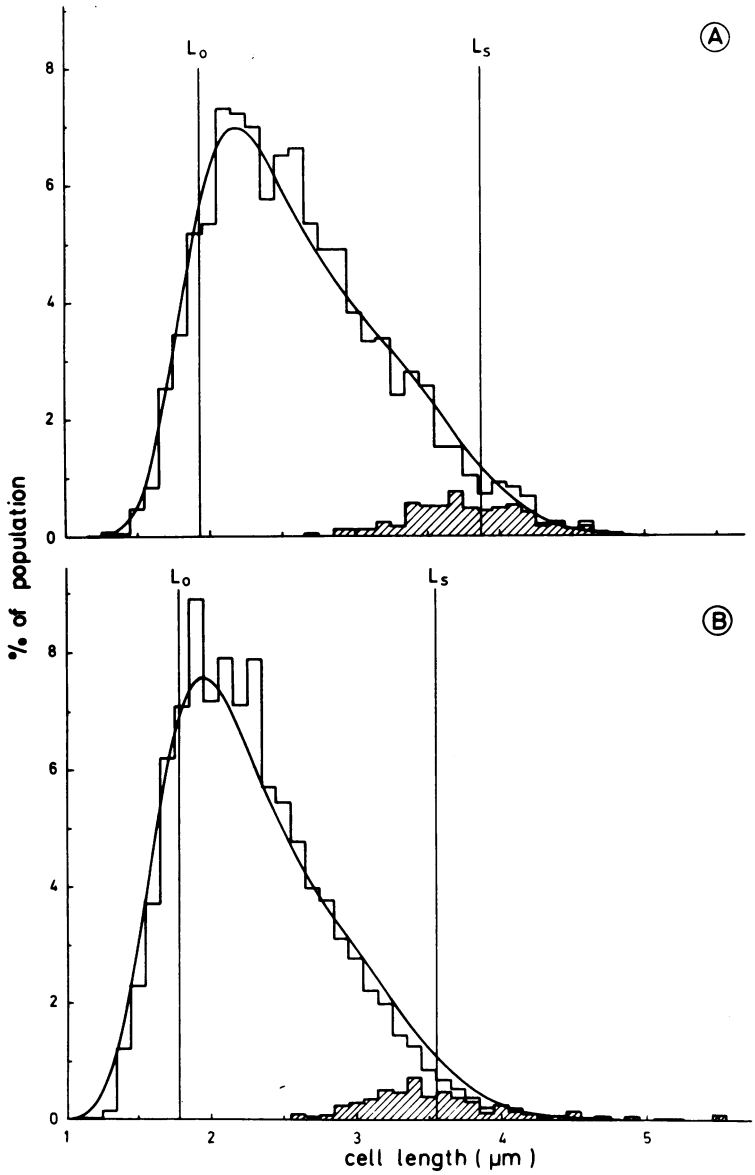

FIG. 2. *Length distributions of E. coli B/r K thy⁻. Histograms: Overall distribution obtained by pooling the distributions of treated cells (0- and 40-min chase; both were corrected by multiplication of lengths with the factor* $m = \bar{L}$ *control cells/*$\bar{L}$ *treated cells,* $0.96 < m < 1.05$*) and the distribution of the untreated control cells. The parameters of the overall distribution are summarized in Table 1. The constricted cells are indicated by the hatched area. Curves: Theoretical distributions calculated from the distribution at birth (mean,* L_0*) and that at cell separation (mean,* L_s*) on the assumption that part of the cell length (L-K) increases exponentially, whereas the other part (k) does not contribute to the growth rate. (A)* $T_D = 90$ *min;* $k = 0.76$ *µm;* $D_{krit} = 3.3\%$*;* $D_{max} = 1.8\%$*. (B)* $T_D = 180$ *min;* $k = 1.12$ *µm;* $D_{krit} = 2.5\%$*;* $D_{max} = 2.9\%$*.*

by means of the equation derived by Collins and Richmond (3, 18). Both a model in which the cell elongates with a constant rate that doubles on the average at length L_b (CV = 15%), and a model in which part of the cell length ($L - K$) increases exponentially whereas the other part (k) does not grow, were tried. The parameter of the linear model that gave the best fit was: $L_b = 2.74$ µm at $T_D = 90$ min and $L_b = 2.40$ µm at $T_D = 180$ min; the parameter of the exponential model that gave the best fit was: $k = 0.76$ µm at $T_D = 90$ min and $k = 1.12$ µm at $T_D = 180$

TABLE 1. *Parameters of overall length distributions*

T_D[a] (min)	No. of cells measured	$\bar{L}$ (μm)	CV (%)	Constricted cells (%)	T[b] (min)	$\bar{L}_T$[c] (μm)	CV (%)	Radioactive cells[d] (%)	C_{max}[e] (min)
90	2,490	2.61	23.5	6.2	7.8	3.76	10.7	57.6	54
180	4,404	2.31	24.3	5.5	13.9	3.33	11.2	38.4	75

[a] T_D, Mass doubling time.
[b] T, Duration of constriction calculated from: $T = T_D \cdot \ln(1 + g)/\ln 2$, in which g = fraction of constricted cells (37).
[c] $\bar{L}_T$, Average length of cells showing constriction.
[d] The percentage of radioactive cells was determined in the sample pulse labeled with [^{3}H]thymidine and covered with emulsion for radioautography (0-min chase sample).
[e] C_{max}, Maximal duration of DNA replication calculated from: $C_{max} = T_D \cdot \ln(1 + h)/\ln 2 - \Delta t$ in which h = fraction of radioactive cells and Δt is the duration of the pulse (22).

TABLE 2. *Estimated average length and CV at different events during the cell cycle*

T_D (min)	Cell birth		Initiation of DNA replication		Initiation of cell constriction		Cell separation	
	L_0 (μm)	CV_0 (%)	L_i[a] (μm)	CV_i[a] (%)	L_c (μm)	CV_c (%)	L_s (μm)	CV_s (%)
90	1.93	12.8	2.39	22.3	3.63	10.0	3.87	9.9
180	1.78	14.3	2.42	14.8	3.30	10.2	3.55	11.4

[a] Corrected for the duration of the pulse (Δt) as follows: $L_i = L_i' - 1/2\ \Delta L$ and $CV_i = 100[(L_i' \cdot CV_i'/100)^2 - (\Delta L)^2/12)]^{1/2}/L_i$, in which L_i' and CV_i' are the incorrected parameters and $\Delta L = \ln 2 \cdot L_i' \cdot \Delta t/T_D$ (see Appendix iii of reference 19).

min. The exponential model gave a better fit at both growth rates. The curves in Fig. 2 represent the best fits calculated for the exponential model.

Length distribution at initiation of DNA replication. For the estimation of length at initiation of DNA replication (L_i), the distribution of nondividing cells that had been fixed after pulse-labeling and washing (0-min chase) was divided into 20 length classes containing about an equal number of cells. For each class the frequency distribution of grains per cell was assessed. The theoretical probability $P(n)$ of observing a cell with n grains is given by the Poisson law (16; see the Appendix of reference 18):

$$P(n) = (1\text{-}S) \cdot e^{-G} \cdot \frac{(G)^n}{n!} + S \cdot e^{-C} \cdot \frac{(C)^n}{n!}$$

where S is the fraction of DNA-synthesizing cells which have on the average C grains per cell, and G is the average number of background grains per cell. This equation was fitted to the observed grain distribution by the method of maximum likelihood (32). The parameters G and C that gave the best fit approximately doubled with increasing length from L_0 to L_s. By linear regression of G and C on length, an improved estimate of the parameter S could be obtained, which is shown as a function of the average length of each length class in Fig. 3 (closed circles).

In *E. coli* B/r K, average lengths at termination of DNA replication (L_f) and at initiation of cell constriction (L_c)coincide (19, 37), and almost all unlabeled, unconstricted cells occur before initiation of DNA replication. Therefore, the theoretical fraction $P(x)$ of labeled unconstricted cells is approximated by (see Appendix ii of reference 19):

$$P(x) = \frac{\Omega(x) - \Xi(x)}{1 - \Xi(x)}$$

in which:

$$\Omega(x) = \int_0^x \omega(y) \cdot dy$$

i.e., the cumulative length distribution at initiation of DNA replication, and:

$$\Xi(x) = \int_0^x \xi(y) \cdot dy$$

i.e., the cumulative length distribution at cell constriction. The above equation, in which the parameters L_i and CV_i [defining $\omega(x)$] were variable and the parameters L_c and CV_c [defining $\xi(x)$] were constant (Table 2), was fitted to the estimated fraction of labeled cells, S, by the method of maximum likelihood (10). The parameters of the distribution at initiation of DNA replication [$\omega(x)$] that gave the best fit (curve in Fig. 3) are given in Table 2.

Length distribution at initiation of cell constriction. For the estimation of length at initiation of cell constriction (L_c), the overall length distribution $\lambda(x)$ (Fig. 2; Table 1) was divided into 10 length classes such that each class contained about an equal number of cells.

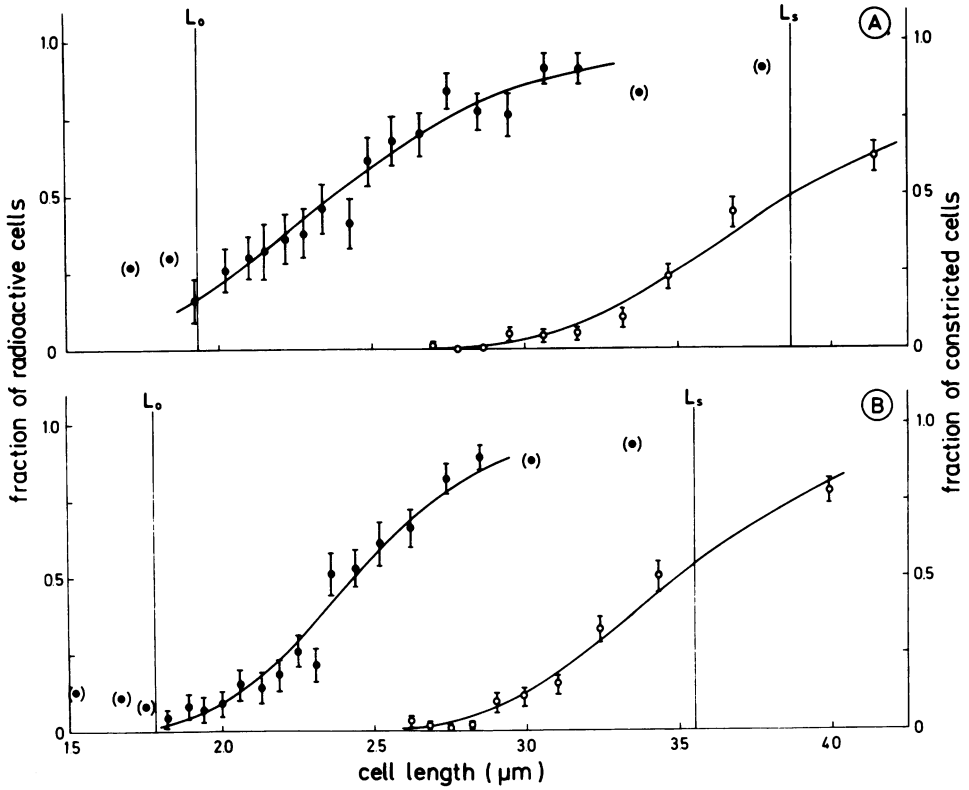

FIG. 3. *Fractions of radioactive and constricted cells per length class. (A) T_D = 90 min. (B) T_D = 180 min. (●) Fractions of radioactive cells in each length class of the distribution of unconstricted cells (0-min chase sample). The curves were calculated assuming; L_i = 2.44 μm, CV = 21.9% (A); L_i = 2.46 μm, CV = 14.6% (B). Fractions within brackets were neglected in the calculation. (○) Fractions of constricted cells in each length class of the overall length distribution. The curves were calculated assuming: L_c = 3.63 μm, CV = 10.0% (A); L_c = 3.30 μm, CV = 10.2% (B). The standard error is given by the bars. Average length at birth (L_o) and at cell separation (L_s) is indicated by the vertical lines.*

The observed fractions of constricted cells in each class are shown in Fig. 3 (open circles) as a function of the average length of that class. Theoretical fractions $P(x)$ are approximated by (see above):

$$P(x) = \frac{\Xi(x) - \Phi(x)}{1 - \Phi(x)}$$

in which:

$$\Phi(x) = \int_0^x \phi(y) \cdot dy$$

i.e., the cumulative length distribution at cell separation. The curves shown in Fig. 3 were obtained by fitting the above equation to the observed fractions by the method of maximum likelihood (10). The parameters of the distribution at initiation of constriction [$\xi(x)$] that gave the best fit are given in Table 2.

Distribution of times between initiation of DNA replication and cell constriction. In the strain of *E. coli* used, a pulse with [^{3}H]-thymidine will label almost all unconstricted cells after initiation of DNA replication, whereas those before this event (i.e., in the B period) remain unlabeled. The kinetics of the appearance of the latter cohort of cells in the constriction "window" of the cell cycle are shown in Fig. 4 (fraction of unlabeled constrictions plot) and has been used to estimate the variability of the U period (time interval between the onset of DNA replication and cell constriction). This was accomplished as follows. Theoretical fractions of unlabeled constricted cells were calculated according to the method of Nachtwey and Cameron (25). This method corrects for the average duration of the constriction process (T period; see Table 1) and assumes a log normal distribution of the U period for computational convenience. In addition, exponential increase of the population during the chase period was taken into account. The theoretical fractions were fitted to the observed ones by the method

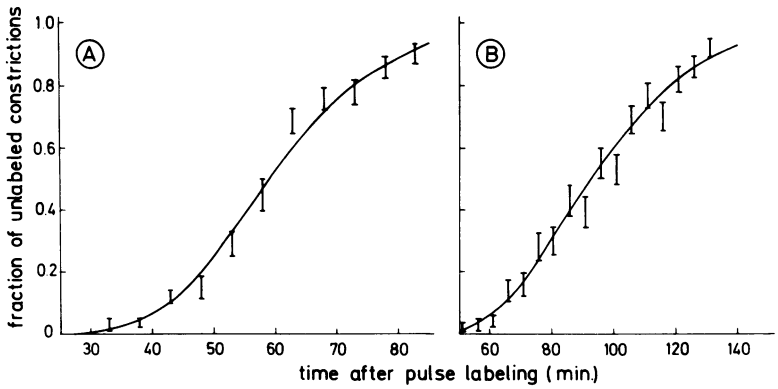

FIG. 4. *Fraction of unlabeled constrictions as a function of time after pulse labeling. (A) T_D = 90 min. (B) T_D = 180 min. The 68% confidence interval for the observed fractions is given by the bars. The curves were calculated assuming a log normal distribution of the U period with parameters: $\bar{U}$ = 55.1 min, CV = 25.4%, T = 7.8 min (A); $\bar{U}$ = 84.5 min, CV = 27.9%, T = 13.9 min (B).*

of maximum likelihood (10). The parameters of the U period that gave the best fit (curve in Fig. 4) are given in Table 3.

Correlation of lengths at initiation of DNA replication and cell constriction. From the estimated average length and CV at initiation of DNA replication and at initiation of cell constriction (Table 2) and from the estimated CV of the U period (Table 3), the correlation coefficient ρ (9) for lengths at both events has been calculated according to the formula:

$$\rho = \frac{(L_i \cdot CV_i)^2 + (L_c \cdot CV_c)^2 - CV_U^2 \cdot (L_c - L_i)^2}{2\, L_i \cdot L_c \cdot CV_i \cdot CV_c}$$

It can be seen (Table 3) that there is a positive correlation in accordance with the model outlined in Fig. 1A. About the same correlation is found on the assumption of either linear or exponential elongation during the U period. The correlation calculated when cell constriction occurs at any length after initiation of DNA replication (the model outlined in Fig. 1B) was about 0.16 (CV_U = 50%) for both T_Ds. This low value is due to the overlap of the length distributions at initiation of DNA replication and at initiation of cell constriction (30).

TABLE 3. *Correlation of length at initiation of DNA replication and at initiation of cell constriction*

T_D (min)	U[a] (min)	CV_U[a] (%)	ρ(lin.)[b]	ρ(exp.)[b]
90	57.5	24.1	0.63–1.00	0.76–1.00
180	89.0	26.3	0.69–0.88	0.69–0.98

[a] Corrected for the duration of the pulse (Δt) as follows: $U = U' + 1/2\ \Delta t$ and $CV_U = 100 \cdot [(U' \cdot CV_U'/100)^2 - (\Delta t)^2/12]^{1/2}/U$ in which U' and CV_U' are the uncorrected parameters.

[b] The 77% confidence interval for the correlation coefficient ρ was calculated by substituting the 95% confidence limit of CV_U and those of the parameters L_i, CV_i, L_c, and CV_c (linear model [lin.]) or the equivalent parameters of the log-transformed distributions of L_i and L_c (exponential model [exp.]) into the equation for ρ mentioned in the text.

DISCUSSION

Some models for the cell cycle. The coordination of chromosome replication and cell division in *E. coli* B/r is described in the Helmstetter-Cooper model as a sequence of three periods I + C + D (11). I is the period of preparation for initiation of chromosome replication during which an initiator complex (replisome; see reference 1) of constant size per initiation event is synthesized at a rate equal to the growth rate; C is the period of chromosome replication, and D is the period occurring after completion of chromosome replication up to the time of cell separation. In *E. coli* B/r K, growing with a doubling time $T_D \leq 60$ min at 37°C, the C period and the D period are constant at 42 and 14 min, respectively (14). With $T_D > 60$ min, the C period (22) or both C and D periods (14) have been reported to increase progressively. The model explains how the growth rate in a particular medium determines the frequency of initiation of chromosome replication, which in turn determines the frequency of cell division C + D minutes later (23); it also explains why at different growth rates a round of chromosome replication is initiated on the average at a constant mass per chromosome origin (5; R. H. Pritchard, Heredity **23**:472, 1978).

In the model of Donachie et al. (6, 15), a single event triggers both a round of chromosome replication and, by a parallel way, a process leading to cell separation after C + D min. The aforementioned event would coincide with the acqui-

sition by the cell of a certain initiation mass (5). Helmstetter (12) hypothesizes that envelope growth rather than cell mass controls the frequency of initiation of DNA replication. In line with this idea, Pierucci (28) assumes that new sites of envelope synthesis are inaugurated coincident with initiation of DNA replication. This latter notion is not inconsistent with our own observations. Radioautographic data on the incorporation of tritiated diaminopimelic acid into the cell envelope of *E. coli* PAT 84 (18) and *E. coli* W7 (Verwer and Nanninga, submitted for publication) show that lateral incorporation sites arise at about the same time that DNA replication starts. In addition, the measurement of length growth in two synchronized substrains of *E. coli* B/r hints at an alteration in length growth around the initiation of DNA replication (24). Though it appears quite reasonable that initiation of DNA replication is related to cell mass or, more specifically, to a process occurring in or at the cell envelope, it has to be admitted that clear-cut evidence is still lacking.

Experimental design and limitations. The above models are founded on biochemical determinations in cell populations. They describe the cell cycle in terms of constants and make no allowance for a distribution of cell cycle parameters. However, the statistical aspects of DNA replication and cell division cannot be neglected on the cellular level due to the probable low number of regulatory molecules, target sites, or both per cell (35). In fact, as pointed out above (see Introduction), the CV of sizes at various cell cycle events and the CV of the periods between them can be used to deduce correlations.

In the present study we have estimated the mean and CV of several parameters (i.e., L_i, L_c, U, C; see Fig. 1) of the cell cycle of *E. coli* B/r at two different slow growth rates. At these growth rates ($T_D > 100$ min), the procaryotic cell cycle resembles the eucaryotic one in showing periods devoid of DNA synthesis (22).

We made a number of assumptions in the analysis of the radioautograms and in the estimation of the parameters L_i, L_c, CV_i, CV_c, and CV_U. We should consider these limitations of our approach in more detail before we discuss the values of the parameters and before we proceed to interprete the coefficient of correlation ρ (L_i, L_c), which we calculate from them.

(i) Although we can measure the dimensions of bacteria quite precisely ($\approx$0.01 μm), the accuracy of our length measurements may be influenced by a variable drying process of the cells prepared by agar filtration. This variation would increase CV_i and CV_c.

(ii) Two sources of variation are inherent to radioautography, both of which tend to inflate CV_i. Variable amounts of radioactivity are incorporated by the cells that initiate DNA replication during pulse labeling. We have corrected L_i, CV_i, U, and CV_U for the duration of pulse labeling (reference 19, appendix iii). This correction was only small and could possibly be omitted. The other source of variation is due to the random decay of tritium. We made use of this variation by fitting a Poisson distribution to the frequencies of grains per cell in each length class.

(iii) The fraction of unlabeled constricted cells was assessed in the electron microscope on the assumption that cells with no or one grain are unlabeled and those with two or more grains are labeled. This procedure inflates CV_U dependent on the average number of background grains.

(iv) Impairment of the radioactive cells by the decay of tritium could retard their progress towards division during the chase, and thus increase CV_U. We are inclined to reject this possibility because of the unaltered doubling time after the pulse. In the calculation of CV_U the T period was assumed to be constant. Distribution of the T period would increase CV_U. However, we found that CV_U is rather insensitive to the duration of the T period (see also Fig. 6 in reference 25).

(v) The formula for ρ (L_i, L_c) gives the exact correlation only if the different distributions relate to the same sample of cells. However, we estimated L_i and CV_i in a sample of cells that are initiating chromosome replication and L_c, CV_c, and CV_U in a sample of constricting cells. The difference of the means of distributions that are defined for different samples is probably small and within the error of measurement.

(vi) In the calculation of ρ (L_i, L_c) we had to assume a relation between cell age and cell size. We considered two simple models: linear and exponential elongation during the U period. Both models gave about the same correlation (Table 3). We have also assumed equal growth rate constants for all cells. Variation of the growth rate will tend to decrease the correlation. However, the CV of the specific growth rate is probably small ($\approx$6%; see reference 7) relative to CV_U and could then be neglected.

Errors in the different parameters have a different effect on ρ (L_i, L_c). The correlation increases with increasing L_i and CV_i but with decreasing L_c, CV_c, and CV_U. Therefore, the various errors cancel each other out to some extent in the formula for the correlation. The 77% confidence interval for ρ (L_i, L_c) in Table 3 has to be understood as an attempt to account for the sources of experimental variation.

Comparison of cell cycle parameters. The values calculated for the C period (Table 1) do not differ significantly from those of the wild-

type strain at similar T_D (19, 22). Thus, the *thy* mutation does not appear to limit the rate of DNA replication, whereas the growth rate does (22). The C period is about the same or shorter than the U period (Table 3). Therefore, on the average, termination of DNA replication precedes or coincides with initiation of visible constriction, as we observed previously (19, 37).

The CV_i of length at initiation of DNA replication (Table 2) is within the range of 15 to 25% reported by Koch (16). The CV_i (22%) found for T_D = 90 min is rather large as compared to that estimated previously by means of a graphic procedure for the wild-type strain growing with T_D = 100 min (CV_i = 16%; see Table 3 of reference 19). When we analyzed the same radioautographic data (19) by means of the procedure outlined above, we found a higher value (CV_i = 21%), similar to that of the *thy* auxotroph at about the same T_D. Therefore, we think that the large difference of CV_i at T_D = 90 min and T_D = 180 min (Table 2) is due to the different growth rates. The large CV_i of size at initiation of chromosome replication that we find (CV_i = 15 to 22%) and the smaller variation in the time (I) between successive initiations reported by Newman and Kubitschek (26; $CV_I \approx 9\%$) are not contradictory to each other, because they apply to different parameters.

From the estimated CV_U of the time interval between initiation of DNA replication and initiation of cell constriction (i.e., 25%; Table 3) and from the reported CV_τ of the interdivision time (i.e., 20%; 21, 29, 31, 33), it can be inferred that the CV of the sum of the B and T periods has to be at least 30 to 35%. The CV_B of age at initiation of DNA replication estimated in synchronized cultures of *E. coli* B/r F is larger (i.e., ≈60%; manuscript in preparation); this implies a negative correlation between the B and U period.

Coordination of DNA replication and cell division. The positive coefficient of correlation ρ between the lengths at which cells initiate DNA replication and initiate visible cell constriction (Table 3) signifies a strong linear relationship between the two variables L_i and L_c. We distinguish between the following possibilities (see Fig. 5). (i) The true ρ equals 1, and it was due to experimental error that we found a

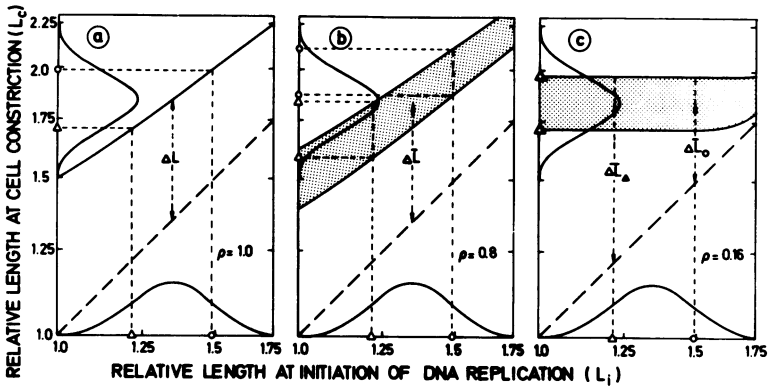

FIG. 5. *Diagrams to illustrate three different ways in which length at initiation of DNA replication (L_i) can be correlated with length at initiation of cell constriction (L_c). Note the use of logarithmic scales which transform the log normal frequency distributions of L_i and L_c (CV, 15% and 10%, respectively) to normal ones. The relationship between L_i and L_c is indicated by the rising curve (A) or by a 68% probability band (B, C; stippled area). (A) Both small (Δ, $\bar{L}_i$ − standard deviation) and large cells (o, $\bar{L}_i$ + standard deviation) at initiation of DNA replication start to constrict after they have elongated with the constant length increment $\Delta L = L_c - L_i$. Length at the onset of constriction is already determined at initiation of DNA replication [the coefficient of correlation ρ (L_i, L_c) = 1.0]. Therefore, the coordination can be called deterministic (see also Fig. 1A). (B) Small (Δ) and large cells (o) at initiation of DNA replication start to constrict after a variable length increment ΔL (CV = 24%). Length at the onset of constriction is not fully determined at initiation of DNA replication [the coefficient of correlation ρ (L_i, L_c) = 0.8]. The coordination can be called probabilistic or stochastic. (C) Both small (Δ) and large cells (o) at initiation of DNA replication start to constrict, on the average, at the same length, $\bar{L}_c$. The average length increment $\Delta\bar{L}$ between both events differs for the two cells. Length at the onset of constriction is hard to determine at initiation of DNA replication [the coefficient of correlation ρ (L_i, L_c) = 0.16]. The coordination can be called independent (see also Fig. 1B). In the construction of the diagrams it has been assumed that constriction can only occur after initiation of DNA replication, i.e., $L_c \geq L_i$, and above the diagonal (broken line) in the plots. Therefore, at large L_i the 68% probability band for L_c converges to the diagonal in Fig. 5C (upward distortion, right upper corner). This dependence causes the low positive value of ρ (see reference 30).*

lower value (see above). The length of a cell at constriction would therefore be predetermined at initiation of DNA replication (Fig. 1A and 5A). Such a coordination can be called deterministic. (ii) The true ρ is slightly less than 1, as we actually estimated. The length of a cell at constriction is, therefore, not fully predictable from its length at initiation of DNA replication, because the length increment ΔL between both events varies (Fig. 1A and 5B). Such a coordination can be called probabilistic or stochastic. (iii) The true ρ is only slightly positive, and it has been inflated by experimental error (see above). The length of a cell at constriction is then "independent" of that at initiation of DNA replication. (In fact, a low correlation arises beforehand when the onset of constriction always occurs after initiation of DNA replication.) In this way there is hardly any coordination (Fig. 1B and 5C). We consider this model improbable because of the confidence interval of 77% which we calculated for ρ (see Table 3).

The high correlation between L_i and L_c doesn't necessarily imply that initiation of DNA replication has a direct effect on the onset of constriction (besides allowing it). It could also reflect the common influence of another event before initiation of DNA replication on both processes. This latter feature is expressed in the model of Donachie et al. (6, 15) and implicitly in the model of Pierucci (28).

The correlation we calculated means that cells that initiate DNA replication at a big size proceed faster to division than cells that initiate at a small size, thus reducing the CV of cell size (homeostasis; see reference 8). Such a mechanism of size control is compatible with our observation that the rate of DNA replication, estimated from the average number of grains above cells engaged in DNA replication, seems to accelerate as cells become bigger (Fig. 5 of reference 19; this paper).

In conclusion, our results suggest that the size of a cell at division is determined in a stochastic way (Fig. 5B) at initiation of DNA replication. Current experiments with synchronized cultures are concerned with the question of to what extent size at initiation of DNA replication is predetermined at birth.

ACKNOWLEDGMENTS

We are grateful to Jos Joosten and Anneke Maagdelijn for helping with the agar filtration, to J. H. D. Leutscher for drawing the figures, to J. Raphaël-Snijer for making the prints, and to E. C. Gräper for typing the manuscript. We thank Wim Voorn for statistical advice, C. L. Woldringh for reading the manuscript, and G. J. Brakenhoff for the computing facilities.

LITERATURE CITED

1. **Bleecken, S.** 1971. Replisome controlled initiation of DNA replication. J. Theor. Biol. **32**:81-92.
2. **Clark, D. J.** 1968. Regulation of deoxyribonucleic acid replication and cell division in *Escherichia coli* B/r. J. Bacteriol. **96**:1214-1224.
3. **Collins, J. F., and M. H. Richmond.** 1962. Rate of growth of *Bacillus cereus* between division. J. Gen. Microbiol. **28**:15-33.
4. **Dix, D. E., and C. E. Helmstetter.** 1973. Coupling between chromosome completion and cell division in *Escherichia coli*. J. Bacteriol. **115**:786-795.
5. **Donachie, W. D.** 1968. Relationship between cell size and time of initiation of DNA replication. Nature (London) **219**:1077-1079.
6. **Donachie, W. D., N. C. Jones, and R. T. Teather.** 1973. The bacterial cell cycle. Symp. Soc. Gen. Microbiol. **23**: 9-14.
7. **Errington, F. P., E. O. Powell, and N. Thompson.** 1965. Growth characteristics of some Gram-negative bacteria. J. Gen. Microbiol. **39**:109-123.
8. **Fantes, P. A.** 1977. Control of cell size and cycle time in *Schizosaccharomyces pombe*. J. Cell Sci. **24**:51-67.
9. **Feller, W.** 1967. An introduction to probability theory and its applications, 3rd ed., vol. 1, p. 236. John Wiley & Sons, Inc., New York.
10. **Finney, D. J.** 1973. Probit analysis, 3rd, ed. Cambridge University Press, London.
11. **Helmstetter, C. E.** 1969. Regulation of chromosome replication and cell division in *Escherichia coli*, p. 15-35. *In* G. M. Padilla, G. L. Whitson, and I. L. Cameron (eds.), The cell cycle. Academic Press, Inc., New York.
12. **Helmstetter, C. E.** 1974. Initiation of chromosome replication in *Escherichia coli*. II. Analysis of the control mechanism. J. Mol. Biol. **84**:21-36.
13. **Helmstetter, C. E., and S. Cooper.** 1968. DNA synthesis during the division cycle of rapidly growing *Escherichia coli* B/r. J. Mol. Biol. **31**:507-518.
14. **Helmstetter, C. E., and O. Pierucci.** 1976. DNA synthesis during the division cycle of three substrains of *Escherichia coli* B/r. J. Mol. Biol. **102**:477-486.
15. **Jones, N. C., and W. D. Donachie.** 1973. Chromosome replication, transcription and control of cell division in *Escherichia coli*. Nature (London) New Biol. **243**:100-103.
16. **Koch, A. L.** 1977. Does the initiation of chromosome replication regulate cell division? Adv. Microb. Phys. **16**:49-98.
17. **Koch, A. L., and M. Schaechter.** 1962. A model for the statistics of the cell division process. J. Gen. Microbiol. **29**:435-454.
18. **Koppes, L. J. H., N. Overbeeke, and N. Nanninga.** 1978. DNA replication pattern and cell wall growth in *Escherichia coli* PAT 84. J. Bacteriol. **133**:1053-1061.
19. **Koppes, L. J. H., C. L. Woldringh, and N. Nanninga.** 1978. Size variations and correlation of different cell cycle events in slow-growing *Escherichia coli*. J. Bacteriol. **134**:423-433.
20. **Kopriwa, B. M.** 1975. A comparison of various procedures for fine grain development in electron microscopic radioautography. Histochemistry **44**:201-224.
21. **Kubitschek, H. E.** 1962. Normal distribution of cell generation rate. Exp. Cell Res. **26**:439-450.
22. **Kubitschek, H. E., and C. N. Newman.** 1978. Chromosome replication during the division cycle in slowly growing, steady-state cultures of three *Escherichia coli* B/r strains. J. Bacteriol. **136**:179-190.
23. **Maaløe, O., and N. O. Kjeldgaard.** 1966. Control of macromolecular synthesis. Benjamin, New York.
24. **Meyer, M., M. A. de Jong, R. Demets, and N. Nanninga.** 1979. Length growth of two *Escherichia coli* B/r substrains. J. Bacteriol. **138**:17-23.
25. **Nachtwey, D. S., and I. L. Cameron.** 1968. Cell cycle analysis. Methods Cell Physiol. **3**:241-250.
26. **Newman, C. N., and H. E. Kubitschek.** 1978. Variation in periodic replication of the chromosome in *Escherichia coli* B/r T T. J. Mol. Biol. **121**:461-471.

27. **Painter, P. R., and A. G. Marr.** 1968. Mathematics of microbial populations. Annu. Rev. Microbiol. **22**:519–548.
28. **Pierucci, O.** 1978. Dimensions of *Escherichia coli* at various growth rates: model for envelope growth. J. Bacteriol. **135**:559–574.
29. **Powell, E. O.** 1958. An outline of the pattern of bacterial generation times. J. Gen. Microbiol. **18**:382–417.
30. **Powell, E. O.** 1964. A note on Koch and Schaechter's hypothesis about growth and fission of bacteria. J. Gen. Microbiol. **37**:231–249.
31. **Powell, E. O., and F. P. Errington.** 1963. Generation times of individual bacteria: some corroborative measurements. J. Gen. Microbiol. **31**:315–327.
32. **Rao, C. R.** 1973. Linear statistical inference and its applications, 2nd ed., p. 366–373. John Wiley & Sons, New York.
33. **Schaechter, M., J. P. Williamson, J. R. Hood, and A. L. Koch.** 1962. Growth, cell and nuclear division in some bacteria. J. Gen. Microbiol. **29**:421–434.
34. **Siegel, S.** 1956. Nonparametric statistics for the behavioral sciences. McGraw-Hill Kogakusha, Ltd., Tokyo.
35. **Spudich, J. L., and D. E. Koshland.** 1976. Non-genetic individuality: chance in the single cell. Nature (London) **262**:467–471.
36. **Weinberger, M., and C. E. Helmstetter.** 1979. Chromosome replication and cell division in plasmid containing *Escherichia coli* B/r. J. Bacteriol. **137**:1151–1157.
37. **Woldringh, C. L., M. A. de Jong, W. van den Berg, and L. Koppes.** 1977. Morphological analysis of the division cycle of two *Escherichia coli* substrains during slow growth. J. Bacteriol. **131**:270–279.